Growth of SiC Films on Si(100) by Electron Cyclotron Resonance Chemical Vapor Deposition Using SiH$_4$/CH$_4$/H$_2$

Chih-Chien Liu and Chiapyng Lee

Department of Chemical Engineering, National Taiwan Institute of Technology, Taipei, Taiwan

Kuan-Lun Cheng and Huang-Chung Cheng

Department of Electronics Engineering, National Chiao-Tung University, Hsinchu, Taiwan

Tri-Rung Yew

Materials Science Center, National Tsing-Hua University, Hsinchu, Taiwan

ABSTRACT

SiC films were deposited on Si(100) substrates by electron cyclotron resonance chemical vapor deposition at 500°C using SiH$_4$/CH$_4$/H$_2$ gas mixtures. The chemical composition and crystalline microstructure were investigated by x-ray photoelectron spectroscopy and cross-sectional transmission electron microscopy, respectively. The film composition and microstructure are correlated to process variables. The deposition mechanism which controls the film characteristics is presented.

Introduction

Silicon carbide (SiC) is an important material for potential applications in photoelectronics, high temperature semiconducting devices, wear resistant coatings, and protective barriers for corrosion or thermal oxidation. All these applications are due to its unique properties such as wide bandgap, high electron mobility, high thermal conductivity, and high melting point. Further, SiC can be used as a thin buffer layer for the growth of diamond films on silicon substrates.[1]

Preparation of this material, especially for hard coating, is usually performed by chemical vapor deposition (CVD) because of its advantage for forming multicomponent, high density, and well-crystallized films on the surface of the desired shape. However, SiC films produced by the CVD method are often not stoichiometric but contain excess silicon or carbon, causing changes in film properties. Therefore, to obtain a suitable chemical composition and crystalline phase for a specific purpose, it is important to understand the mechanism which determines the optimal process parameters for the deposition of the desired film. However, for the deposition of crystalline β-SiC, a high reaction temperature, usually higher than 1000°C,[2] is necessary and limits the application of CVD.

Recently, a few researchers have tried to decrease the deposition temperature of crystalline β-SiC films by using electron cyclotron resonance chemical vapor deposition (ECR-CVD). Diani *et al.*[3] synthesized monocrystalline β-SiC (3C-SiC) by ECR-CVD at temperatures above 800°C. Katsuno *et al.*[4] reported the growth of microcrystalline SiC thin films at 300°C without identifying the crystalline phase. In previous work[5] the deposition of stoichiometric microcrystalline β-SiC at 500°C by ECR-CVD from mixtures of SiH$_4$, CH$_4$, and H$_2$ has been successfully achieved. However, detailed characterization the composition and microstructure of the SiC film deposited by ECR-CVD and film-formation mechanism have not been published. The purpose of this work is to correlate the variation of film chemical composition and crystalline microstructure to the deposition parameters. The mechanism which governs the correlation is proposed.

Experimental

Substrates used were (100) oriented, p-type silicon wafers with a resistivity of 5-15 Ω-cm, and were cut into 12 × 30 mm size. The substrates were cleaned *ex situ* by a modified spin-etching method[6] to provide a hydrogen-terminated silicon surface and prevent surface oxidation during air exposure.[7]

SiC films were deposited in a commercial Plasma-Quest Model 357 electron cyclotron resonance reactor using CH$_4$/SiH$_4$/H$_2$ gas mixtures. Details of the ECR-CVD reactor were described in a previous publication.[5] The total pressure was kept constant at 20 mTorr. The CH$_4$/SiH$_4$ flow ratio was varied by changing CH$_4$ flow rate while keeping SiH$_4$ flow rate at 5 sccm. The effect of microwave power was investigated by keeping the CH$_4$ and SiH$_4$ flow rates at 5 and 2.5 sccm, respectively. The flow rate of H$_2$ was kept constant at 100 sccm. The deposition time was 30 min in all cases.

XPS analyses were performed in a VG Microtech MT-500 spectrometer. The spectrometer was equipped with a hemispherical analyzer and all x-ray photoelectron spectroscopy (XPS) data presented here were acquired using the Mg K$_\alpha$ x-rays (1253.6 eV). Peak positions were calibrated with respect to the C 1s peak at 284.6 eV from the adventitious hydrocarbon contamination.

The crystalline structure of the deposited film was examined in a JEOL 200CX STEM. The samples used for cross-sectional transmission electron microscopy (XTEM) inspection were cut into 3 × 6 mm size. The XTEM is a destructive analysis technique to observe the deposited film with electron beams perpendicular to the wafer surface normal. As XTEM can be used to observe the deposited film and the film/substrate interface simultaneously, it becomes the most direct and precise way to determine the crystalline phase and lattice constant of the deposited films.

Results

The independent process variables in our deposition process that determine the film composition and microstructure are the following, (*i*) methane to silane flow ratio (CH$_4$/SiH$_4$) as measured in relative flow rates, and (*ii*) the microwave power. In this section we present the influences of these parameters on film composition and microstructure.

Experiments with varied CH$_4$/SiH$_4$ flow ratios were carried out at a fixed SiH$_4$ flow rate of 5 sccm with the CH$_4$ flow rate varying from 1 to 50 sccm. The microwave power was kept constant at 1200 W. Figure 1 shows high resolution XPS spectra of Si 2p peaks for various CH$_4$/SiH$_4$ flow ratios. The binding energies for Si and SiC are 100 and
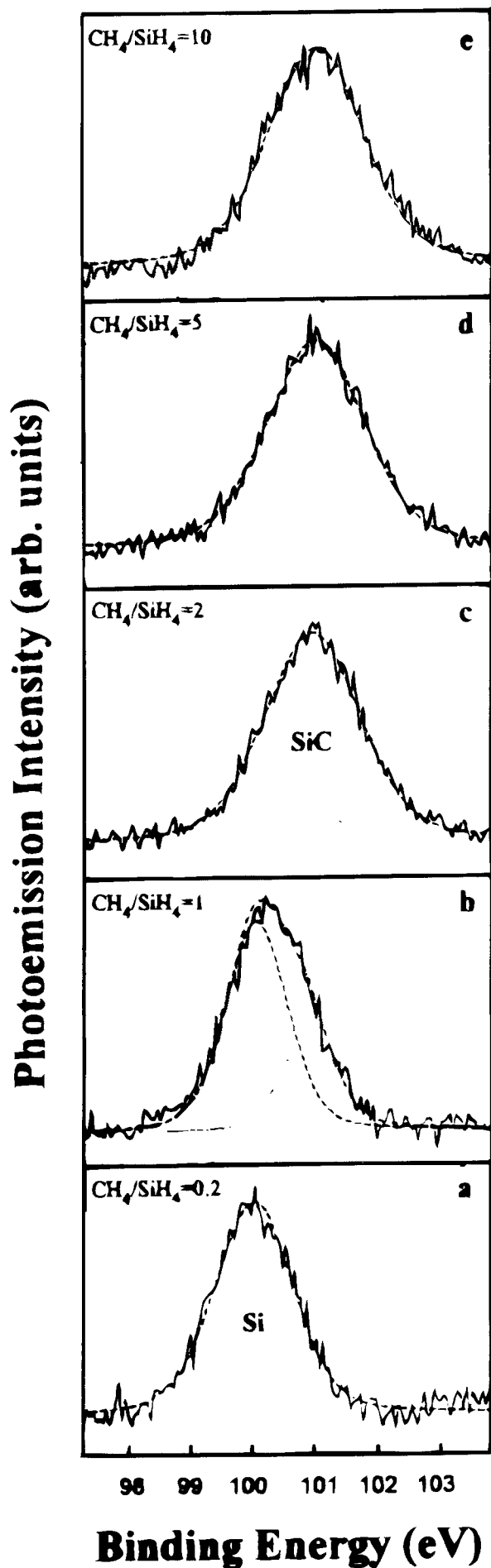
Fig. 1. Deconvolution of Si2p XPS core level peaks for the films deposited at various CH_4/SiH_4 flow ratios.
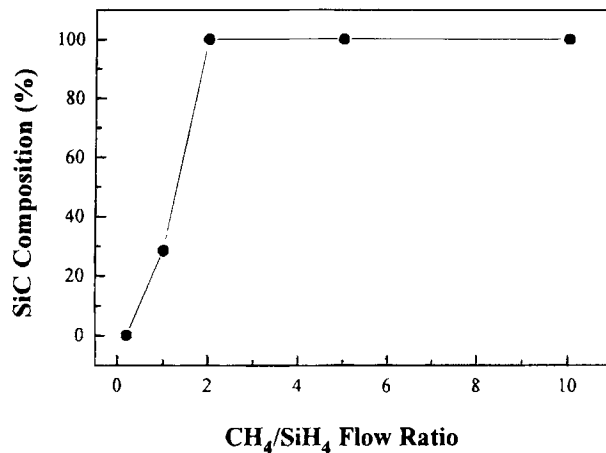

Fig. 2. SiC composition in the films deposited at various CH_4/SiH_4 flow ratios.

101.3 eV, respectively. The binding energies measured here are slightly deviated from those obtained by other researchers,[8] but an energy difference Δ-SiC (C 1s-Si 2p) of 182.2 eV is in agreement with those reported.[8,9] Figure 1a shows that only Si is formed at a CH_4/SiH_4 flow ratio of 0.2. When the CH_4/SiH_4 flow ratio is increased to 1 (Fig. 1b), the Si 2p peak shifts to a binding energy between elemental Si and SiC because of overlap of peaks. The Si 2p XPS spectrum shown in Fig. 1b could be deconvoluted into Si (100 eV) and SiC (101.3 eV) by assuming Gaussian-Lorentzian type distributions. The composite curves of the two components match the experimental spectra well. From Fig. 1, it can be found that as the CH_4/SiH_4 flow ratio is increased to 2 and higher, only SiC is formed. The film compositions were estimated from the peak area of each component after normalizing with the respective relative sensitivity factor.[10] According to Fig. 1, changes in the SiC composition of the film as a function of the CH_4/SiH_4 flow ratio can be obtained, as shown in Fig. 2.

Figure 3 shows cross-sectional TEM (XTEM) dark-field and bright-field micrographs with electron diffraction patterns of the films grown at different CH_4/SiH_4 flow ratios. Figure 3a indicates that at a CH_4/SiH_4 flow ratio of 1 (same as in the case of the flow ratio of 0.2), the deposited films on Si are of polycrystalline Si (poly-Si) determined by the ring spacing of the electron diffraction pattern. The grains shown in the dark-field image (Fig. 3a) were of Si, since they are taken from the Si<111> ring in diffraction pattern. The Si 2p peak (Fig. 1b) shows the existence of SiC which could hardly be observed in the diffraction pattern of Fig. 3a. This may be because SiC is of an amorphous form and the amount of SiC is too small to be monitored by XTEM. When the CH_4/SiH_4 flow ratio was increased to 2, the microcrystalline β-SiC could be deposited as shown in Fig. 3b. Using the spot diffraction pattern of <110> Si zone in Fig. 3b as a reference, the film is identified to be zinc-blende structure with a lattice constant of 0.434 ± 0.006 nm, which is identical to that of bulk β-SiC.[5] The grains shown in the dark-field image are of SiC since they were taken from the SiC<111> ring in the diffraction pattern. At CH_4/SiH_4 flow ratios above 2, amorphous SiC (a-SiC) was observed. The typical XTEM micrograph of amorphous SiC is shown in Fig. 3c which was deposited at a CH_4/SiH_4 flow ratio of 10. Therefore, a CH_4/SiH_4 flow ratio of 2 is crucial for crystalline β-SiC formation according to our aforementioned results at various flow ratios. It is not clear why a thin amorphous layer exists between the deposited film and substrate in Fig. 3a and b.

Experiments with varied microwave powers were conducted at a fixed SiH_4 flow rate of 5 sccm. The CH_4/SiH_4 flow ratio was kept constant at 2. Figure 4 shows the high-resolution XPS spectra of Si 2p peaks for different microwave powers. The shift phenomenon of Si 2p peaks is similar to that observed in Fig. 1 for different flow ratios.
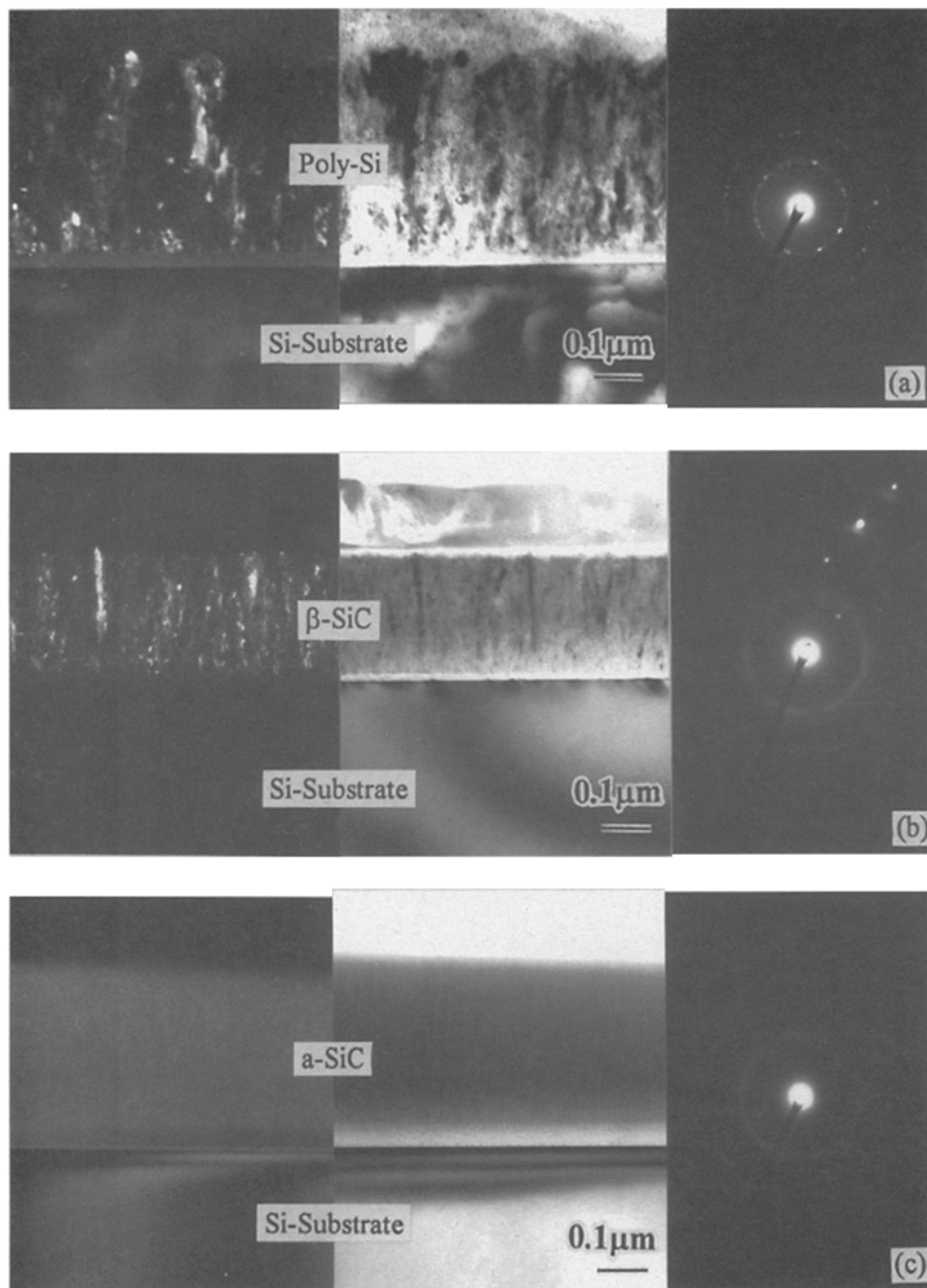
Fig. 3. Dark-field and bright-field XTEM micrographs and diffraction patterns of the films deposited at 500°C, a microwave power of 1200 W, and a CH_4/SiH_4 flow ratio of (a) 1, (b) 2, and (c) 10.

When the microwave power is increased from 300 to 1500 W, the Si 2p peak shifts from the elemental Si to the SiC. This indicates that the amount of SiC in the deposited thin film increases with the microwave power. Figure 4a shows that only Si is formed at 300 W. The Si 2p XPS spectra for 500 and 800 W (Fig. 4b and c) also could be deconvoluted into Si and SiC. However, when the microwave power is increased to 1200 W and higher (Fig. 4d and e), only SiC is deposited. Figure 5 shows the effect of microwave power on the composition of SiC in the films.

Microstructures of the films grown at different microwave powers were investigated and the results are shown in Fig. 6. When the microwave power is 300 W, Fig. 6a indicates that only polycrystalline Si is deposited. At a microwave power of 500 W, the film which is composed of amorphous SiC and embedded polycrystalline Si grains (a-SiC + poly-Si) is deposited. This result is shown in Fig. 6b. However, when the microwave power is increased to 1200 W and higher, microcrystalline β-SiC films are deposited as shown in Fig. 6c. Therefore, a sufficient microwave power is required to deposit microcrystalline β-SiC. It is also unclear why an amorphous layer exists at the interface in Fig. 6a-c.

Discussion

In the present work we have studied the effects of CH_4/SiH_4 flow ratio and microwave power on the growth of microcrystalline β-SiC at 500°C by ECR-CVD using XPS and XTEM.

We clearly observe in Fig. 3 that when the CH_4/SiH_4 flow ratio is varied from 0.2 to 10, the crystalline phase is changed from the polycrystalline silicon to the microcrystalline β-SiC, and finally to the amorphous silicon carbide. In Fig. 6, when the microwave power increases from 300 to 1500 W, the film microstructure is changed from the polycrystalline Si to the polycrystalline silicon grains embedded in amorphous SiC, and finally to the microcrystalline β-SiC. Therefore, to obtain a suitable chemical composition and microstructure for a specific purpose, it is important to understand the mechanism that governs the film formation.

Under the condition of excess hydrogen as in this study, the plasma chemistry of SiH_4/H_2 has been studied by Shieh *et al.,*[11,12] and that of CH_4/H_2 by Hsu[13] and Mitomo *et al.*[14] Shieh *et al.*[11,12] suggested that SiH_4 decomposes in the plasma to produce H_2 and more reactive precursor species
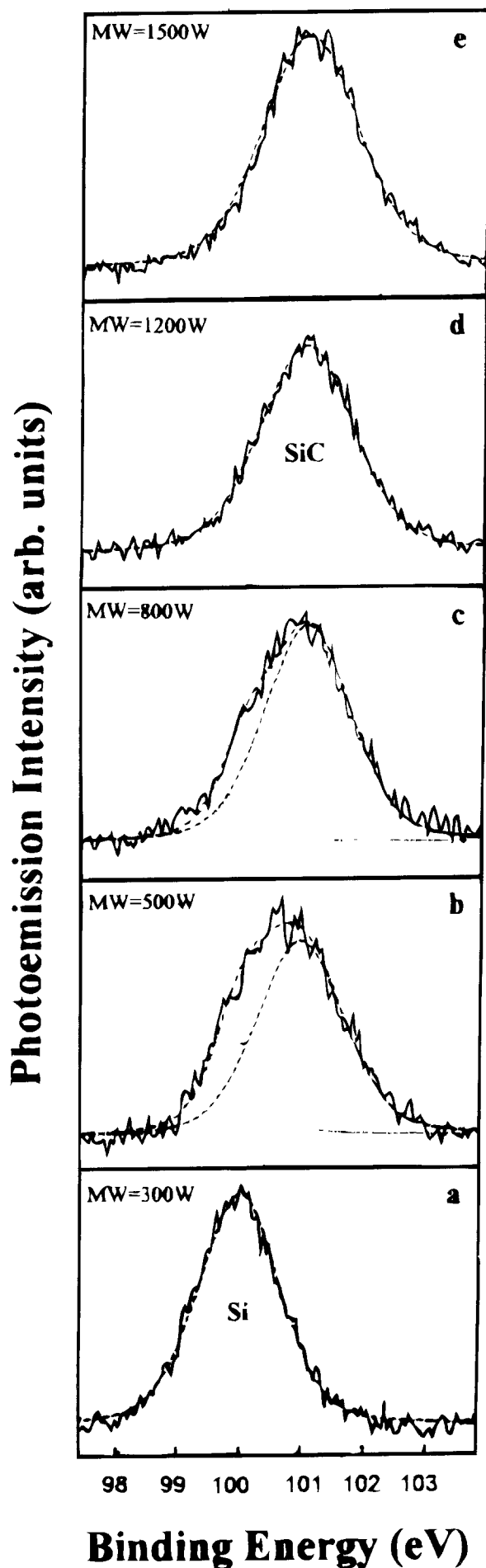
Fig. 4. Deconvolution of Si2p XPS core level peaks for the films deposited at various microwave powers.
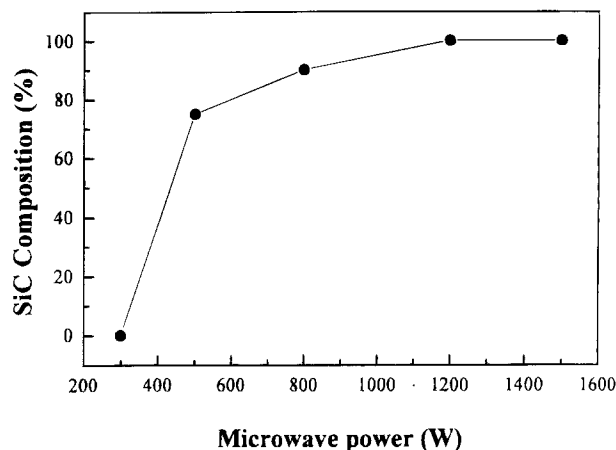

Fig. 5. SiC composition in the films deposited at various microwave powers.

SiH_x (x = 0, 2, 3), and the major radicals for the deposition of silicon should be SiH_x (x = 0, 2, 3). Besides, Hsu[13] studied the microwave plasma chemistry of CH_4/H_2 by molecular beam mass spectroscopy (MBMS) and found that CH_4 can react with the hydrogen atom to form CH_3 which can be converted subsequently into C_2H_2 in excess H-atom. Mitomo *et al.*[14] used Fourier transform infrared (FTIR) spectroscopy to study the effect of various carbon feed gases. Their reports also confirm the result of Hsu[13] on the formation of C_2H_2. For low pressure CVD amorphous SiC growth, a mechanism has been proposed by Hong *et al.*[15,16] and is described as follows. Si_2H_6 decomposes in the gas phase to form SiH_2 which reacts with C_2H_2 in two paths, (*i*) a reaction of the gaseous SiH_2 with C_2H_2 adsorbed on the surface and (*ii*) a gas-phase reaction between gaseous SiH_2 and gaseous C_2H_2 to form another intermediate product, most plausibly, $SiH_3\equiv CH$.

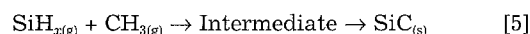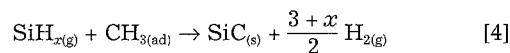Based on the above discussion, the most probable film formation mechanism for the present work is proposed as follows

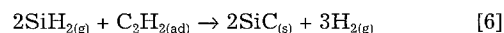1. Under the plasma environment, silane decomposes in the gas phase to form SiH_x (x = 0, 2, 3) and H_2

$$SiH_{4(g)} \rightarrow SiH_{x(g)} + \frac{4-x}{2} H_{2(g)} \qquad [1]$$
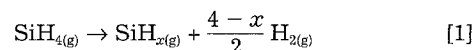
2. Methane can react with the hydrogen atom to form methyl and a rapid conversion from methyl to acetylene can be sustained in excess H atom

$$H_{(g)} + CH_{4(g)} \rightarrow H_{2(g)} + CH_{3(g)} \qquad [2]$$

$$2CH_{3(g)} \rightarrow C_2H_{2(g)} + 2H_{2(g)} \qquad [3]$$
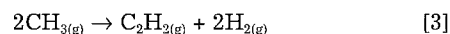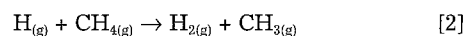
3. SiH_x may react with CH_3 in two paths (*i*) a reaction of the gaseous SiH_x with CH_3 adsorbed on the surface and (*ii*) a gas-phase reaction between gaseous SiH_x and gaseous CH_3 to form an intermediate product

$$SiH_{x(g)} + CH_{3(ad)} \rightarrow SiC_{(s)} + \frac{3+x}{2} H_{2(g)} \qquad [4]$$

$$SiH_{x(g)} + CH_{3(g)} \rightarrow Intermediate \rightarrow SiC_{(s)} \qquad [5]$$

4. SiH_2 may also react with C_2H_2 in two paths (*i*) a reaction of the gaseous SiH_2 with C_2H_2 adsorbed on the surface and (*ii*) a gas-phase reaction between gaseous SiH_2 and gaseous C_2H_2 to form an intermediate product, most plausibly $SiH_3\equiv CH$ as proposed by Hong *et al.*[15]

$$2SiH_{2(g)} + C_2H_{2(ad)} \rightarrow 2SiC_{(s)} + 3H_{2(g)} \qquad [6]$$

$$SiH_{2(g)} + C_2H_{2(g)} \rightarrow Si_3HC\equiv CH_{(g)} \rightarrow SiC_{(s)} \qquad [7]$$

But the real mechanism still needs to be proved by mass spectroscopy analysis which is an interesting subject for future work.
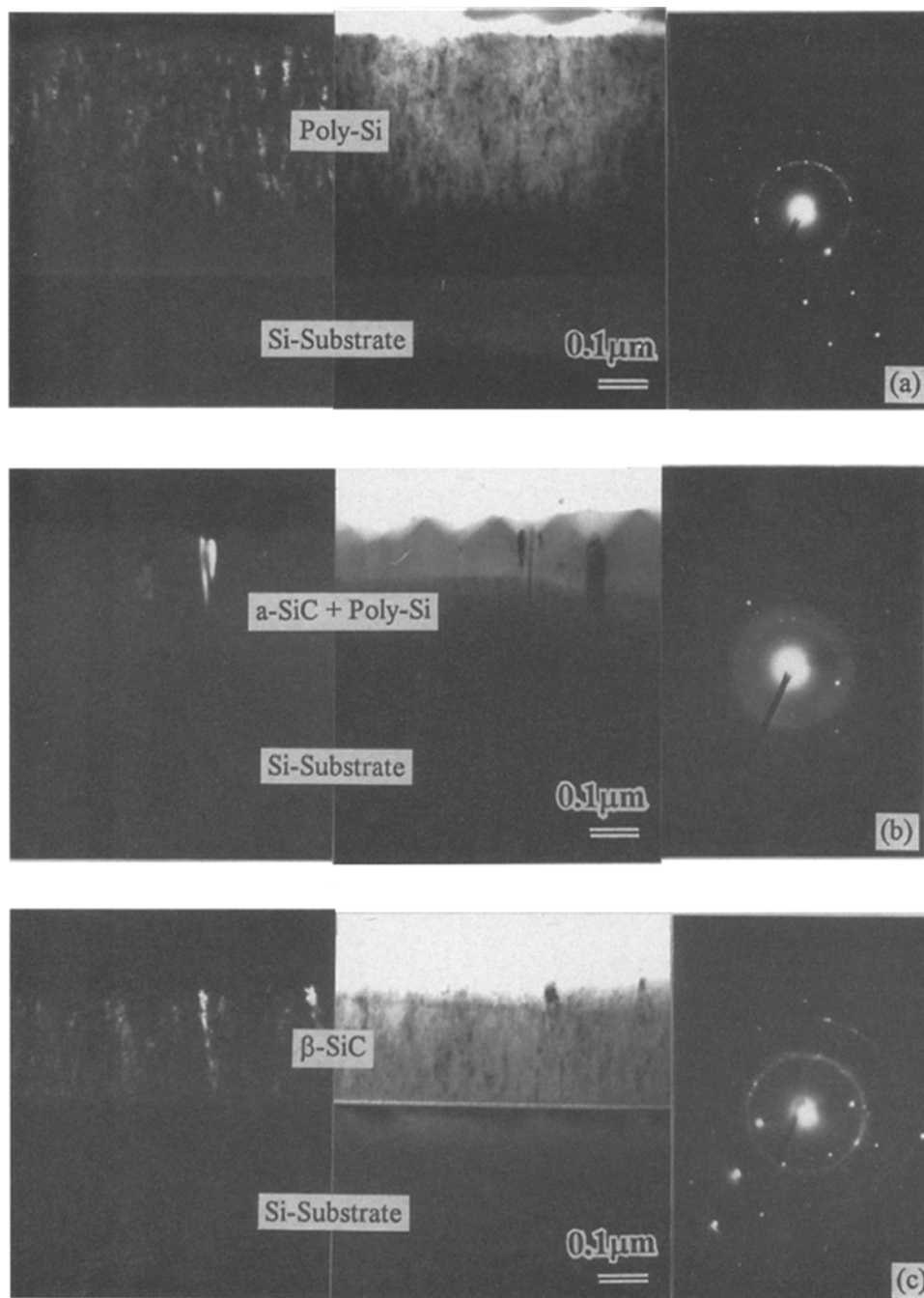
Fig. 6. Dark-field and bright-field XTEM micrographs and diffraction patterns of the films deposited at 500°C, a CH_4/SiH_4 flow ratio of 2, and a microwave power of (a) 300, (b) 500, and (c) 1500 W.

With the mechanism proposed above, the formation of various type films at different CH_4/SiH_4 flow ratios and microwave powers can be explained as follows. Since the bond energies of Si—H and C—H are about 320 and 410 kJ/mol,[17] respectively, this suggests that most likely the SiH_4 has a higher dissociation efficiency than CH_4. At CH_4/SiH_4 flow ratios below 2, since the concentration of CH_4 is too low, the decomposition reaction of SiH_4 (Eq. 1) should dominate and result in many SiH_x radicals. The SiH_x radicals adsorb onto the Si surface where they decompose and polycrystalline silicon is deposited (Fig. 3a). At a CH_4/SiH_4 flow ratio of 2, relatively larger amounts of the CH_4 are added into the system. The amounts of CH_3 radicals and C_2H_2 are comparable with that of SiH_x, so that steps 3 and 4 of the mechanism could occur to form SiC with a suitable growth rate (0.159 nm/s) and the stoichiometric microcrystalline β–SiC film is obtained (Fig. 3b). However, at CH_4/SiH_4 flow ratios above 2, it is possible that the growth rate is too high (0.389 nm/s at CH_4/SiH_4 = 10) so that the SiC deposited on the Si substrate surface does not have sufficient time to

arrange in an orderly fashion. Therefore, amorphous SiC is obtained (Fig. 3c). The XPS data (Fig. 1 and 2) also show the change of film type from poly-Si to SiC and the variation of film composition.

When the microwave power is as low as 300 W, the deposited film is still poly-Si (Fig. 6a) even at a CH_4/SiH_4 flow ratio of 2. That is still because the energy needed for SiH_x formation is lower than that of CH_4 decomposition and the energy is enough for the subsequent decomposition of SiH_x to occur. However, at 500 W microwave power, the energy supplied by plasma may be enough for the dissociation of CH_4 so that most SiH_x radicals can react with CH_3 radicals and C_2H_2 to form SiC, but may not be enough for surface rearrangement. However, 500 W maybe is still too low to produce a sufficient amount of CH_3 radicals and C_2H_2. The residual SiH_x adsorbs onto the Si surface and results in the growth of poly-Si grains. Therefore, amorphous SiC and embedded poly-Si grains can be observed in the film (Fig. 6b). As the microwave power is increased to 1200 W and higher, the supplied energy is sufficient for both the

formation of radicals and the crystallization of amorphous SiC into microcrystalline β-SiC (Fig. 6c). The XPS data (Fig. 4 and 5) also show the change of film type from poly-Si to SiC and the variation of film composition.

Conclusion

XPS and XTEM were used to study films deposited by ECR-CVD using $SiH_4/CH_4/H_2$ mixtures. When the CH_4/SiH_4 flow ratio were varied from 0.2 to 10, the crystalline phase of films varie from polycrystalline silicon to the microcrystalline β-SiC, and finally to amorphous silicon carbide. As the microwave power increases from 300 to 1500 W, the film microstructure change from polycrystalline Si to polycrystalline silicon grains embedded in amorphous SiC, and finally to microcrystalline β-SiC. A film-formation mechanism is proposed to explain the correlation between film characteristics (composition and microstructure) and process variables.

Acknowledgment

REFERENCES

1. E. G. Wang, *Physica B*, **185**, 85 (1993).
2. R. F. Davis, G. Kelner, M. Shur, J. W. Palmour, and J. A. Edmond, *Proc. IEEE*, **79**, 677 (1991).
3. M. Diani, J. L. Bischoff, L. Kubler, and D. Bolmont, *Appl. Surf. Sci.*, **68**, 575 (1993).
4. M. Katsuno, T. Futagi, Y. Ohta, H. Mimura, and K. Kitamura, *ibid.*, **70/71**, 675 (1993).
5. C. C. Liu, C. Lee, K. L. Cheng, H. C. Cheng, and T. R. Yew, *Appl. Phys. Lett.*, **66**, 168 (1995).
6. C. H. Chen, C. M. Wan, and T. R. Yew, *ibid.*, **62**, 3126 (1993).
7. P. J. Grunthaner, F. J. Grunthaner, R. W. Fathauer, T. L. Lin, M. H. Hecht, L. D. Bell, and W. J. Kaiser, *Thin Solid Films*, **183**, 197 (1989).
8. I. Kusunoki and Y. Igari, *Appl. Surf. Sci.*, **59**, 95 (1992).
9. P. A. Taylor, M. Bozack, W. J. Choyke, and J. T. Yates, *J. Appl. Phys.*, **65**, 1099 (1989).
10. D. Briggs and M. P. Seah, *Practical Surface Analysis by Auger and X-Ray Photoelectron Spectroscopy*, John Wiley & Sons, New York (1983).
11. M. D. Shieh, C. Lee, and T. R. Yew, *This Journal*, **141**, 3584 (1994).
12. M. D. Shieh, C. Lee, C. H. Cheng, T. R. Yew, and C. Y. Kung, *Appl. Phys. Lett.*, **63**, 1252 (1993).
13. W. L. Hsu, *J. Appl. Phys.*, **72**, 3105 (1992).
14. T. Mitomo, T. Ohta, E. Kondoh, and K. Ohtsuka, *ibid.*, **70**, 4532 (1991).
15. L. S. Hong, Y. Shimogaki, Y. Egashira, and H. Komiyamd, *This Journal*, **139**, 3653 (1992).
16. I. S. Hong, Y. Shimogaki, and H. Komiyama, *J. Phys. C*, **1**, 2 (1991).
17. I. S. Butler and J. F. Harrod, *Inorganic Chemistry: Principles and Applications*, p. 274, The Benjamin/Cummings Publ. Co., Redwood City, CA (1989).